

# Air-Lubricated Bearings with Capillary Air-Feeder Holes

By

Tokio SASAKI and Haruo MORI

Department of Mechanical Engineering

(Received November 30, 1956)

## Abstract

Capillary air-feeder holes of which each one is considered to possess the ability of two restrictions in series have been applied to air-lubricated bearings at high speed. It has been concluded by the experiment that the air-lubricated bearing, having capillary air-feeder holes located in diametral symmetry, can be operated in quite a stable state and with an extremely small coefficient of friction—which conclusion coincides perfectly with the value calculated by Petroff's equation. Then it is recognized that the air-lubricated bearing with capillary air-feeder holes is the one which has the smallest friction and good dynamic stability.

## 1. Introduction

As reported previously,<sup>(1)</sup> the dynamic stability of air-lubricated bearings operating at high speed can be improved a great deal by locating the primary restrictor, like a nozzle, before the air-feeder hole in the air supply line against the secondary restriction through which the supply air flows into the bearing clearance just after the air-feeder hole, because the two restrictions in series produce an automatic controllability which maintains the shaft center in non-eccentric state by changing the intermediate pressure between the two restrictions accordingly as the bearing clearance at the air-feeder hole changes.

When a capillary hole is applied as the air-feeder hole, it becomes the primary nozzle and at the same time it also performs the activity of the secondary restriction just before the bearing clearance.

In order to obtain more stable air-lubricated bearings than those with two restrictors located apart which had been reported previously, it is considered desirable to locate a number of capillary air-feeder holes at equal spacings on the circumference of bearing as these holes are considered to cooperate each

other and control probable vibrations of the shaft at high speed.

In this paper, it is described how the air-lubricated bearings with capillary air-feeder holes are designed and investigated by measuring the coefficient of friction and the quantity of air-flow.

### 2. Design of Capillary Air-Feeder Holes

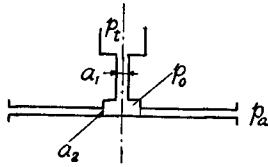


Fig. 1. A path of air-flow at an air-feeder hole

We shall inspect a path of air-flow as shown in Fig. 1. The air with constant supplying pressure  $p_t$  passes through the primary restrictor in the sectional area  $a_1$  and flows into the secondary restrictor in the sectional area  $a_2$ . Then, the pressure  $p_t$  descends to the intermediate pressure  $p_0$  and the value of  $p_0$  can be controlled by the ratio  $a_2/a_1$  as shown in Fig. 2.<sup>(1)</sup> Denoting  $r_0=$

radius of air-feeder hole acting as the primary restriction,  $r_c=$ radius of air-feeder hole acting as the secondary restriction, and  $h=$ bearing clearance at the air-feeder hole,  $a_1$  and  $a_2$  are given by  $\pi r_0^2$  and  $2\pi r_c h$ . Since  $r_0$  and  $r_c$  take constant values in some of the air-lubricated bearings, the change of the ratio  $a_2/a_1$  depends on the change of the clearance  $h$ . In Fig. 2, it is obvious that  $p_0$  decreases or increases depending upon the increase or decrease of the clearance  $h$  and the largest rate of change of  $p_0$  occurs at the inflection point of the  $p_0 \sim h$  curve. In our previous report, the inflection point is given theoretically by  $a_2/a_1=1.56$  and  $p_0/p_t=0.63$  and estimated experimentally to exist in the range of  $a_2/a_1=1.1 \sim 1.6$  and  $p_0/p_t=0.81 \sim 0.63$  when  $p_0=2.0 \sim 4.0$  kg/cm<sup>2</sup> (absolute pressure).

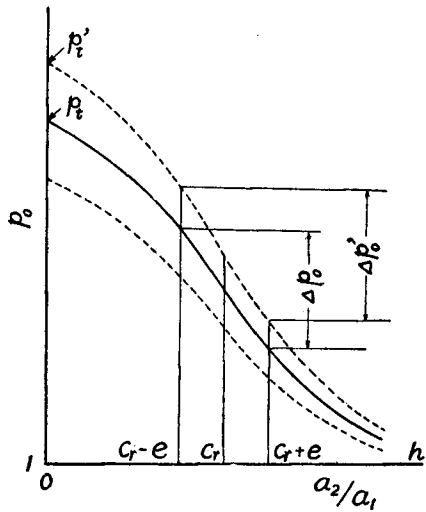


Fig. 2. Characteristic curves of intermediate pressure  $p_0$  to change of clearance

Now, let us consider a design of an air-lubricated bearing in which the air-feeder holes described above are located at equal spacings around the circumference of a bearing bush as shown in Fig. 3. When the center of the shaft is displaced from the center of the bearing, the pressure  $p_0$  at each air-feeder hole increases or decreases corresponding to the decrease or increase of bearing clearance against the same value of  $p_t$  which is the constant supplying pressure to the air-lubricated bearing. Then the difference of pressure distribution in the bearing, which can

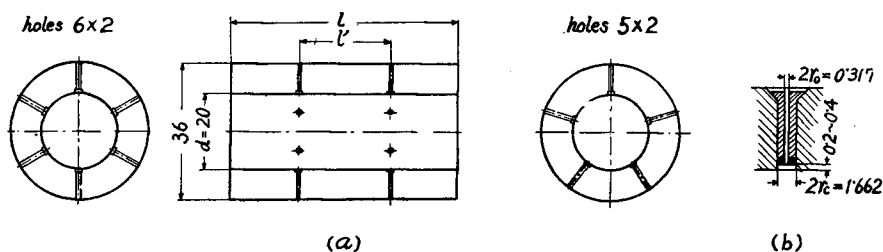


Fig. 3. (a) Bearing bushes for test  
(b) Section of an air-feeder hole

be considered to be locally proportional to each  $p_0$  at the air-feeder hole<sup>(2)</sup>, produces a load carrying ability in the reverse direction of the displacement of the shaft. This fact is more obvious in Fig. 2 in which  $c_r$  is taken as the radial clearance and  $e$  as the displacement of the shaft center. Taking a pair of air-feeder holes which are upper and lower holes in the direction of displacement of the shaft, the pressure difference  $\Delta p_0$  may be produced as the clearances at these holes change to  $c_r + e$  or  $c_r - e$  from  $c_r$  and produces the difference of pressure distribution which supports the bearing load. It is obvious from Fig. 3 that the pressure difference  $\Delta p_0$  increase as the displacement  $e$  increases, and a larger pressure difference  $\Delta p_0'$  occurs for the same value of  $e$  when the supplying pressure  $p_t$  increases to  $p_t'$ . Consequently, if  $p_t$  is taken to be sufficiently large for the bearing load, the difference of pressure distribution becomes large so that the displacement of the shaft may be held into the state of nearly non-eccentric rotation. Moreover, since the change of  $e$  has a great influences upon  $\Delta p_0$ , a strong self-centering ability can be obtained. To increase this ability, it is desirable to choose the concentric state of shaft and bearing at a state in which  $\frac{dp_0}{dh}$  becomes maximum. This means that the inflection point of  $p_0 \sim h$  curve in Fig. 2 is to be given at  $h = c_r$ , and thus the design of an air-feeder hole for the given clearance  $c_r$  can be determined by the following formula :

$$\frac{2\pi r_0 c_r}{\pi r_0^2} = 1.1 \sim 1.6 \quad (1)$$

if  $r_0 = r_0$ ,

$$\frac{2c_r}{r_0} = 1.1 \sim 1.6 \quad (1')$$

### 3. Conditions of Experiment

The balance beam testor reported in our previous paper<sup>(3)</sup> is used to investigate the frictional characteristics of the air-lubricated bearing with capillary air-feeder holes and the experimented bearing bushes are shown in Fig. 3. The

main dimensions of these bushes and the bearing clearances, which are schemed to adapt these bushes to several shafts, are shown in Table 1. The air-feeder

Table 1. Diametral clearance  $2c_r$  in  $\mu$

Bush		Shaft		diameter mm				
$d$ mm	No. of holes	$l$ mm	$l'$ mm	20.157	19.968	19.933	19.912	19.823
20.247	5×2	60	24	90				
20.017	6×2	60	24		49	83	(105)	
19.998	5×2	40	16		(30)	65	86	(175)
19.997	6×2	40	16		(29)	64	85	(174)

hole is shown in Fig. 3 (b). Substituting the measured values of  $r_0$  and  $r_c$  in this figure into Eq. (1), the most suitable range of bearing clearance for this air-feeder hole can be given by

$$2c_r = 33.4 \sim 48.4 \mu.$$

In this range of clearance, the most suitable value should be taken larger as the supplying pressure  $p_t$  increases<sup>(1)</sup>. Moreover, it should be noted that there may be favorable ranges of clearance equally taking low friction on both sides of the most suitable clearance.

#### 4. Experimental Results

Among the group of various bearing clearances, unsuitable clearances, at which the bearing bush can not float perfectly in a static condition by supplying compressed air, are found and these belong to two groups in which the diametral clearances are smaller than  $30\mu$  or larger than  $108\mu$ . These unsuitable clearances are distinguished in the brackets in Table 1. In this experiment, the group of diametral clearances suitable for the design of the air-feeder holes, at which frictional resistance is quite low, exists in the range of from  $2c_r = 49\mu$  up to  $90\mu$ . This range is rather larger than that expected from the data mentioned before. Some

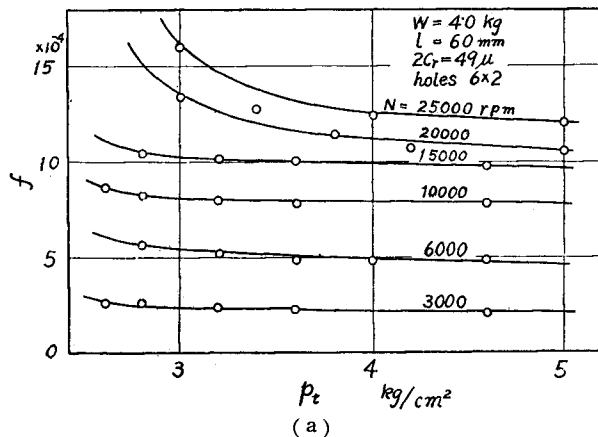


Fig. 4. Relations between coefficient of friction  $f$  and air supplying pressure  $p_t$  ( $l=60\text{mm}$ )

examples of the frictional coefficient  $f$ , measured by increasing supplying pressure  $p_t$  steppedly under the condition of revolving speed  $N$  from 3000 rpm up to 25000 rpm, are shown in Fig. 4 and Fig. 5. Fig. 4 is the case in which the bearing load  $W=4.0$  kg and the bearing length  $l=60$  mm, and Fig. 5 is the case in which  $W=4.1$  kg and  $l=40$  mm. In both cases, the extremely small coefficient of friction of  $10^{-4}$  order is obtainable when the pressure  $p_t$  increases and becomes over a certain value, thereafter the value of  $f$  shows only a little decrease depending upon the increase of  $p_t$ . This

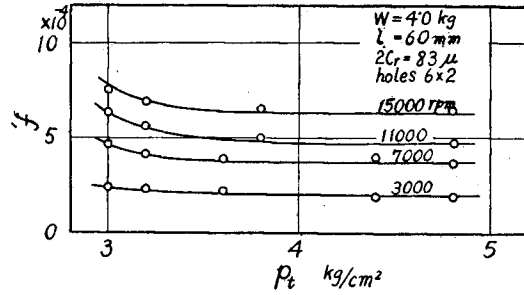


Fig. 4 (b)

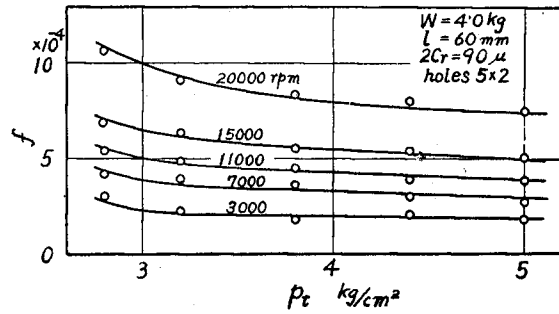
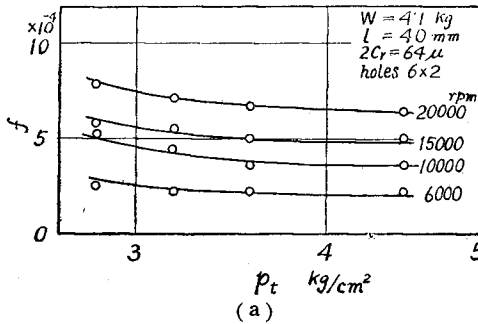
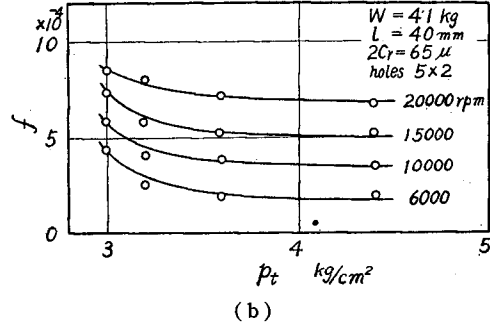


Fig. 4 (c)



(a)



(b)

Fig. 5 Relations between coefficient of friction  $f$  and air supplying pressure  $p_t$  ( $l=40$  mm)

fact, as mentioned previously, shows nothing but the fact that, if the pressure  $p_t$  comes up to a necessary value to float the bearing bush against the bearing load, the increase of  $p_t$  thereafter is used only to reduce the displacement of the shaft center which remains slightly. This operating character is quite different from the air-lubricated bearing with one air-feeder hole in the loading side of the bearing bush reported previously<sup>(3)</sup>. In Fig. 4, comparing (b) with (a) in which the number of air-feeder hole are  $6 \times 2$  (refer Fig. 3 (a)) and  $2c_r=49 \mu$ , (b) is the case in which  $2c_r$  increased up to  $83 \mu$  which is considered rather too large in comparison with the suitable value mentioned above. But in this case

also the operating state of the bearing is very stable and the frictional coefficient takes a little smaller value than that in (a). This decrease of frictional coefficient is considered to depend on the fact that if the centers of the shaft and bearing become almost concentric the coefficient of friction may be given by Petroff's equation;

$$f = 2\pi^2 \left( \frac{d}{2c_r} \right) \frac{\mu N}{p'} = 2\pi^2 \frac{\mu l N d^2}{2c_r W} \quad (2)$$

and  $f$  is considered reversely proportional to diametral clearance. In the above equation,  $p' = \frac{W}{ld}$  and  $\mu$  = viscosity of air. It is also obvious by Eq. (2) that the frictional coefficient  $f$  is proportional to rotational speed  $N$  and bearing length  $l$  and inversely proportional to bearing load  $W$ .

Comparing Fig. 4 (c) which is the case having two rows of five air-feeder holes with (b). which is the case having two rows of six holes and similar value of clearance as the former, the number of holes seems to influence little on the frictional resistance. This fact is also obvious when Fig. 5 (a) is compared with (b). Consequently, it can be concluded in general that the number and location of air-feeder holes are important only as a means to bring about the floating state of the bearing and have no influences directly on the value of friction after the floating state of bearing is attained.

Comparing Fig. 5 (a) and (b) with Fig. 4 (b) and (c), the bearing bushes of the formers, inspite of its smaller diametral clearances as  $64\mu$  and  $65\mu$  than  $83\mu$  and  $90\mu$  of the latter bushes, have smaller coefficient of friction than the bushes of the latters. This is due, as seen from Eq. (2), to the fact that the influence of bearing length  $l$  reduced to 40mm from 60mm is superior to that of the decrease of bearing clearance. Now, denoting,  $f_{min}$

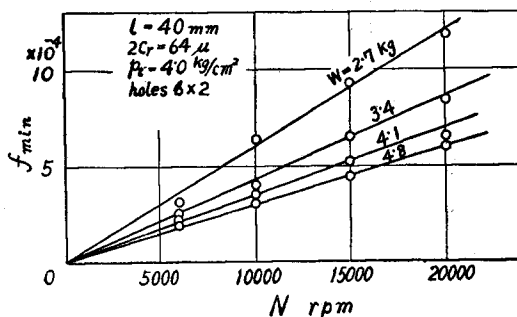


Fig. 6. Relation between  $f_{min}$  and rotational speed  $N$

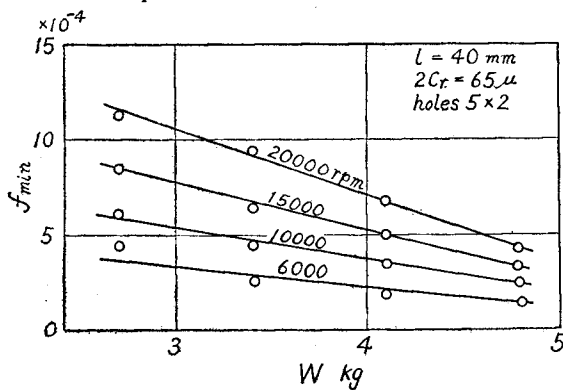


Fig. 7. Relation between  $f_{min}$  and bearing load  $W$

as the value of  $f$  which has become almost constant by increasing the supplying pressure  $p_t$  sufficiently, Fig. 6 shows the relation between  $f_{min}$  and  $N$ , Fig. 7 the relation between  $f_{min}$  and  $W$ , and Fig. 8 the relation between  $f_{min}$  and  $2c_r$ . The linear relations shown in these figures indicate altogether the tendencies seen in Eq. (2).

Therefore, it becomes more obvious when a figure is drawn, as shown in Fig. 9, by taking coordinates of  $f_{min}$

in vertical and  $\left(\frac{d}{2c_r}\right)\left(\frac{\mu N}{p'}\right)$  in horizontal. All experimental data distribute, as

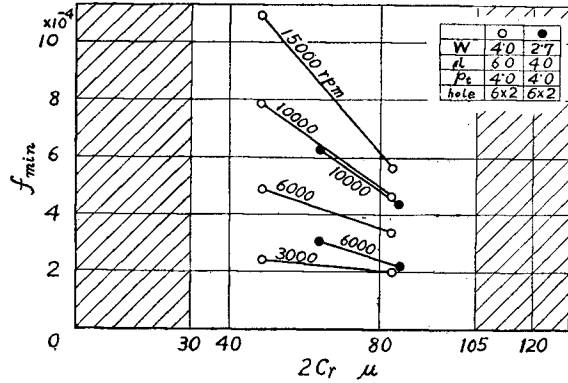


Fig. 8. Relation between  $f_{min}$  and diametral clearance  $2c_r$

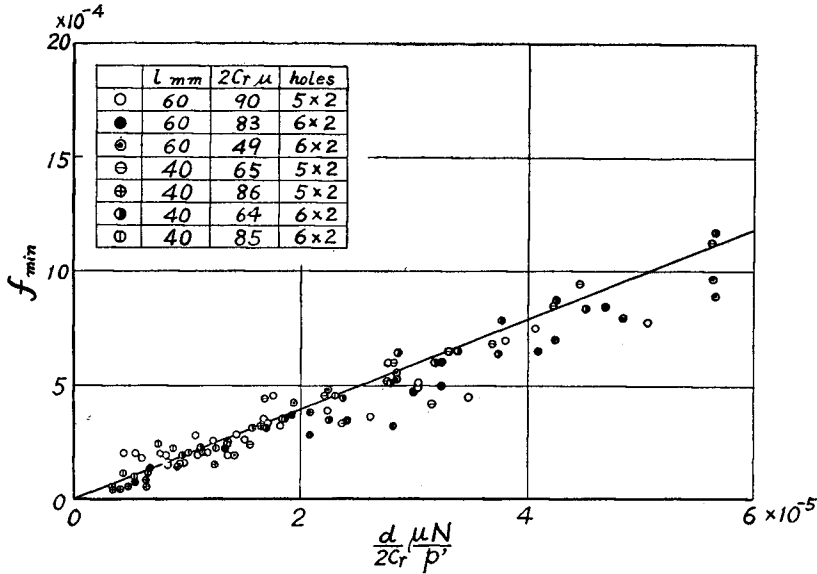


Fig. 9. Diagram of minimum friction  $f_{min}$  versus  $\frac{d}{2c_r} \cdot \frac{\mu N}{p'}$

seen obviously in Fig. 9, along the theoretical line drawn by Eq. (2). This coincidence between the experimental data and theoretical line points out the fact that the shaft floats perfectly by air film in the bearing bush and rotates in very stable manner without any vibration and metallic contact in spite of high speed rotation and absence of oil. Moreover, it is to be noted that the coefficient of friction is almost zero at  $N=0$  when these experimental data are extrapolated. This par-

ticular property has never been seen in the air-lubricated bearings with an ordinary air-feeder hole, which had been reported before. Consequently, it can be concluded that the air-lubricated bearing with capillary holes is the perfect one which can operate in a very stable state with extremely slight friction even at high speed rotation.

When the number of air-feeder holes is reduced successively and the location of air-feeder holes becomes unsymmetric as shown in Fig. 10 above, the frictional coefficient  $f_{min}$  does not change so much in the range of less than 15000rpm, but the load can not be applied to the bearing from an arbitrary direction. The relation between the air-feeder holes and the loading direction is shown in Fig. 10 above. As the rotational speed of the shaft becomes more than 20000rpm,  $f_{min}$  increases rapidly owing to the shortage and unsymmetric location of air-feeder holes. This fact depends on the reduction of controllability of vibration. Moreover, when the number of holes decreases to less than  $3 \times 2$ , the supplying pressure  $p_t$  should be increased greatly. Considering the facts mentioned above, it is most suitable to locate symmetrically the air-feeder holes in the circumference of the bearing bush.

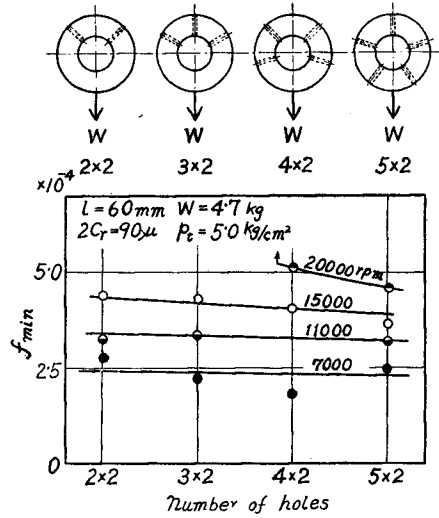


Fig. 10. Influence of decrease of air-feeder holes upon  $f_{min}$

Thus, the value of the supplying pressure is to be discussed in application. Denoting the most suitable pressure as  $p_{tmin}$ , in the case of the air-lubricated bearing with an ordinary air-feeder hole  $p_{tmin}$  could be determined exactly by using the convex characteristic curves of relation between frictional coefficient and supplying pressure<sup>(3)</sup>, but it is difficult to determine exactly in the case of these bearings. Therefore, in this study,  $p_{tmin}$  is assumed to be the value of  $p_t$  above which the coefficient of friction  $f$  becomes almost constant after the initial depression according to the increase of  $p_t$ . Fig. 11 and Fig. 12 show the relation between  $p_{tmin}$  and the bearing load  $W$  or the rotational speed  $N$  in

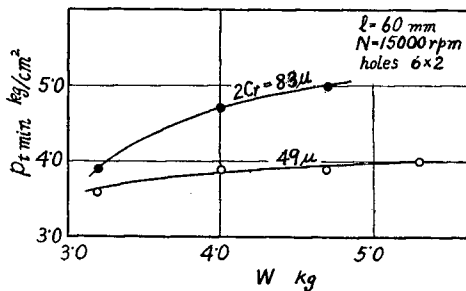


Fig. 11. Relation between suitable pressure  $p_{tmin}$  and bearing load  $W$

Fig. 11 and Fig. 12 show the relation between  $p_{tmin}$  and the bearing load  $W$  or the rotational speed  $N$  in



the case of  $l=60\text{mm}$ , and it is seen from these figures that  $p_{t\text{min}}$  increases as  $W$ ,  $N$  or  $2c_r$  increases. Considering as  $p_{t\text{min}}/p'$ , the value more than 10 is necessary to be taken at  $N=15000\text{rpm}$  even in the case of  $2c_r=49\mu$  at which  $p_{t\text{min}}$  takes small values. It is rather a large value compared with

the air-lubricated bearing reported previously. The influence of the bearing clearance  $2c_r$  upon  $p_{t\text{min}}$  is seen more obviously in the case of  $l=40\text{mm}$  in Fig. 13 compared with the case of  $l=40\text{mm}$  in Fig. 12. That is,  $p_{t\text{min}}$  increases gradually as the rotational speed increases at  $2c_r=64\mu$ , on the contrary, it increases rapidly at  $2c_r=85\mu$ . Since the higher the supplying pressure, the stronger the self-aligning ability of the shaft center and the controllability of vibration, the requirement for higher supplying pressure is considered that it originates in the

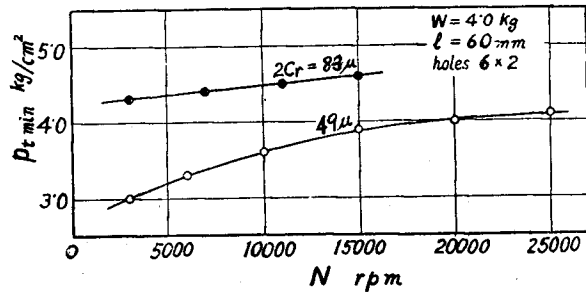


Fig. 12. Relation between suitable pressure  $p_{t\text{min}}$  and rotational speed  $N$  ( $l=60\text{mm}$ )

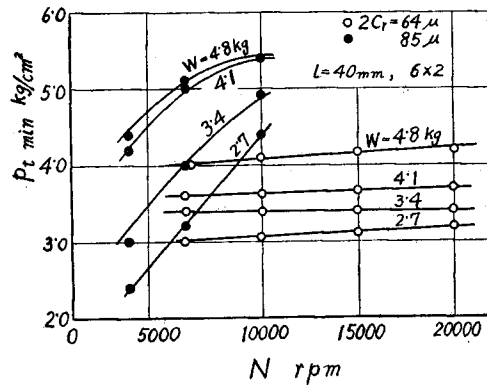


Fig. 13. Relation between suitable pressure  $p_{t\text{min}}$  and rotational speed  $N$  ( $l=40\text{mm}$ )

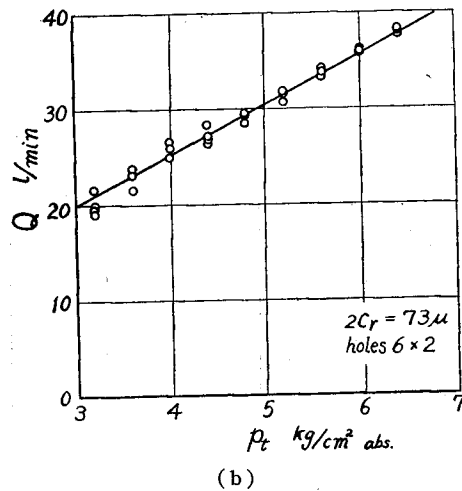
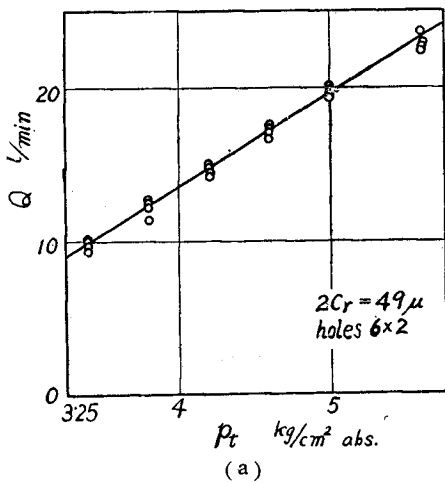


Fig. 14. Relation between quantity of air-flow  $Q$  and supplying pressure  $p_t$

inferiority of dynamic stability. Therefore, the operating state of  $2c_r=85\mu$  is inferior to  $2c_r=64\mu$  concerning dynamic stability in spite of having smaller coefficient of friction as described before. In view of this point,  $2c_r=85\mu$  is too large to be taken and unsuitable for the air-feeder holes designed in this experiment.

The quantity of air-flow  $Q$  is shown in Fig. 14. It increases proportionally to the increase of  $p_t$ , and comparing (a) and (b) in Fig. 14 it is obvious that air flows more plentifully as the bearing clearance increases. In the experimental results, the quantity of air-flow is not affected by the rotational speed.

### 5. Consideration of Experimental Results

It is clarified in the experimental results that, if the rotational shaft is kept in an almost non-eccentric state by applying the suitable supplying pressure  $p_{tmin}$ , the coefficient of friction can be given by Petroff's equation (2) independently of the supplying pressure  $p_t$ . Then, though the coefficient of friction becomes larger by the decrease of the bearing clearance as shown in Fig. 4 (a) and (b) or by the increase of the bearing length as shown in Fig. 4 and Fig. 5, these increases of friction should not be understood as the deterioration of the operating character of bearing because these increases may be explained theoretically to be reasonable. Concerning the influence of the bearing clearance, as discussed in Fig. 13, the diametral clearance of more than  $85\mu$  is considered to be unsuitable to the air-feeder holes designed in this experiment and inferior in the dynamic stability. It can be concluded in this experiment that the bearing clearances of  $2c_r=49\mu$ ,  $64\mu$  and  $65\mu$  are suitable. These values deviate to the larger side over the range of  $2c_r=33.4\sim 48.4\mu$  which has been expected to be suitable. But this range is presumed by experimental results concerning the position of the inflection point of characteristic curve of  $p_0$  as shown in Fig. 2, and it can be considered that a favorable operating state may be obtainable also at the bearing clearance corresponding to the linear part of the characteristic curve of  $p_0$  which exists in wide range on both sides of the inflection point. Therefore, if the range of numerical value of the right side in Eq. (1) is expanded to  $1.0\sim 2.2$  corresponding to the linear part mentioned above, the suitable range of  $2c_r$  becomes  $30.4\sim 66.7\mu$  and this includes the clearances used in the experiment,  $49\mu$ ,  $64\mu$  and  $65\mu$ . Concerning the design of the air-feeder hole, since the operating state becomes worse in the cases of small clearances and the difficulty is little when the clearance becomes too large comparing with the cases of small clearances, it is considered suitable to choose a larger numerical value of the right side of Eq. (1) within its range and take 1.4. Namely, Eq. (1) becomes

$$r_0^2/r_c = 1.43c_r \quad (3)$$

and the dimensions of the air-feeder hole,  $r_0$  and  $r_c$ , can be determined by using Eq. (3) for the bearing clearance  $c_r$  as the given condition. Although the clearance in practical use does not coincide with the value calculated by Eq. (3), the operation of shaft has no trouble if the bearing clearance satisfies the condition of  $2\pi r_c c_r / \pi r_0^2 = 1.0 \sim 2.2$ . Substituting  $r_0 = r_c$  into Eq. (3),  $r_0 = 1.43c_r$  is obtained. Therefore, if the drilling of capillary hole is possible, straight capillary holes under the condition of  $r_0 = 1.43c_r$  may be applied instead of the air-feeder holes which consist of two diameters in this experiment.

## 6. Conclusions

- (1) If the suitable design of the air-feeder hole is applied, the air-lubricated bearing with capillary air-feeder holes can be operated in quite a stable state even at high speed rotation with extremely small coefficient of friction—which coincides perfectly with the value given by Petroff's equation.
- (2) The air-feeder hole should be designed to satisfy the condition of  $r_0^2/r_c = 1.43c_r$  if the hole consists of two diameters as in this experiment, and the condition of  $r_0 = 1.43c_r$  if the hole is straight without step. In practical use, a good operating state can be obtained in the range of  $2r_c c_r / r_0^2 = 1.0 \sim 2.2$ .
- (3) The air supplying pressure  $p_t$  is necessarily to be more than the value of  $p_t/p' = 10$ , and should be increased as the rotational speed and the bearing clearance increase.

## References

- (1) T. Sasaki and H. Mori: "On the Characteristics of Air-Lubricated Bearing (Succeeding Report)", Memoirs of Faculty of Engineering, Kyoto University, Vol. 16, No. 2, Apr., 1954, p. 71.
- (2) T. Sasaki and H. Mori: "Theory of Air-Lubricated Journal Bearing", Transactions of Japan Society of Mechanical Engineers, Vol. 19, No. 86, 1953, p. 45.
- (3) T. Sasaki and H. Mori: "On the Characteristics of Air-Bearing", Memoirs of Faculty of Engineering, Kyoto University, Vol. 13, No. 1, Jan., 1951, p. 21.